NanOQTech

Nanoscale Systems for Optical Quantum Technologies

Grant Agreement No: 712721
Start Date: 1st October 2016 - Duration: 36 months

D3.1 Nano-resonators

Deliverable:	D3.1
Work package:	WP3 Opto-electrical and opto-mechanical hybrid systems
Task:	3.3 Eu3+ nano-mechanical oscillators
Lead beneficiary:	CNRS
Type:	Report
Dissemination level:	Public
Due date:	30 September 2017
Actual submission date:	13 September 2017
Author(s):	Signe Seidelin (CNRS-IN)

This project has received funding from the European Union's Horizon 2020 research and innovation programme under grant agreement No 712721.

Version history

Version	Date	Author(s)	Description
V1	3/09/2017	S. Seidelin (CNRS-IN) Y. Le Coq (CNRS-SY)	First draft
V2	13/09/2017	S. Seidelin (CNRS-IN) and Philippe Goldner (CNRS-CP)	Submission to EC

Copyright Notice

Disclaimer

Table of Contents

Deliverable description

This deliverable consists in a report on the fabrication of nano-resonators described under task 3.3 in WP3. The report contains three main parts: preparatory theoretical considerations (simulations and calculations in order to optimize the geometry and design); actual fabrication (description of employed techniques and description of achieved resonators); optimization of a cryogenic and optical environment for testing the resonators.

Introduction and context

The study of mechanical resonators belongs to the field of optomechanics [1], which emerged experimentally about a decade ago, when several groups started to investigate the techniques required to actively cool a macroscopic mechanical oscillator down to its ground state. The combination of active and traditional cryogenic cooling techniques was intensively pursued and allowed 6 years ago for the very first time to place a mechanical system in its quantum ground state [2, 3]. One way to study the resonators in or close to the quantum ground state, is to couple it to a two-level system, and interact with the resonator via this system. One particularly interesting way to achieve this is to use “strain-coupling”, first demonstrated in 2014 with a semi-conductor nanowire [4]. This strain-coupling can also be used in a rare-earth crystal resonator: In such a resonator, the vibrations, which can be induced deliberately by means of a piezo actuator or result from the Brownian motion due to a finite temperature (or even from the zero-point energy position fluctuations), generate a mechanical strain. This strain influences the electronic properties of the impurity (here, rare-earth ions), as a consequence of the modification of the electronic orbital distributions. The oscillations of the crystal are therefore mapped onto the energy levels of the impurity, which in turn gives rise to a change in the optical frequency of the photons absorbed and emitted. The corresponding strain mediated coupling strength is higher than what can be achieved with any realistic external forces. What is particularly appealing about these integrated hybrid mechanical systems is that some of them may approach or even enter the strong coupling regime [5]. In this regime, the hybrid coupling strength exceeds the decoherence rates of both the mechanical resonator and the impurity (which, according to context, is the decoherence rate of either an electronic transition or a transition between spin states).

Theoretical considerations

Prior to the actual fabrication of the resonators, careful theoretical considerations based on calculations and simulations have been essential, in order to optimize the geometry and design (for achieving maximum coupling, obtain suitable read-out mechanisms etc.). This work has been carried out in a collaboration by three partners of the NanOQTech consortium: AU, CNRS-SY and CNRS-IN. A part of the results discussed in this report have been jointly published in a theoretical research article in Physical Review A [6]. We will in the following summarize the most essential information obtained from this work.

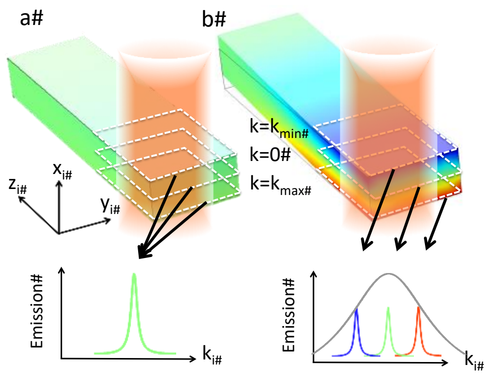

Figure 1 Inhomogeneous broadening due to strain. Blue colours correspond to a compressed material, and red colours to extended material, whereas green corresponds to zero strain. The laser beam is illustrated by a vertical orange cylinder. The strain on the ith ion, ki, depends on its vertical position.

In order to develop a resonator design based on $Eu^{3+}:Y_2SiO_5$ for studying strain-coupled optomechanics, several challenges must be faced. First, the atomic structure make it very challenging to observe single ions (narrow absorption linewidth, weak oscillator strength, and often no closed transitions). We therefore decided to investigate the possibility of using not single ions, but spectral holes imprinted in the structure to which couple the mechanical motion. This is indeed possible, but the fact that an ensemble of ions is involved, adds an inhomogeneous broadening of the lineshape due to the strain arising from mechanical motion. As illustrated in figure 1, the emission line broadens under applied strain (the shift in frequency is denoted by k). In order to overcome this challenge, we developed a theoretical protocol allowing for a dispersive coupling between the edge of a spectral hole and a detuned laser which actually exploits this broadening. More precisely, when the resonator vibrates, the slope of the edge of the spectral hole will oscillate periodically. The coupling will be read-out be observing a phase shift of a laser traversing the resonator. The details of the coupling mechanism are given in ref. [6], including a protocol for “functionalizing” the spectral hole in order to optimize the coupling.

Parameters obtained from simulations

One of the practical consequences of coupling to an ensemble of ions is that laser needs to interact with a large number of ions, making a micrometre scale resonator more suitable, at least for the initial experiments during which the detection efficiency has not yet been fully optimized. For the first prototypes, based on the simulations, we therefore opted for the following parameters: a single-clamped cantilever with the dimensions $100 \times 10 \times 10\ \mu m^3$ interacting with a laser beam traversing the cantilever near its fixed end for maximum strain as illustrated in fig. 1. The cantilever which consists of Y_2SiO_5 (which has a Young Modulus of 135 GP) with an effective mass of 1.1×10^{-11} kg, and of which the first excited mechanical mode vibrates at 890 kHz. The cantilever contains a 0.1 % doping of Eu^{3+} ions, with a $^7F_0 \rightarrow {}^5D_0$ transition centered at 580 nm and with a linewidth of $\Gamma = 2\pi \times 122$ Hz at T=3 K. For our simulations, we used a power of 1 mW and a hole width of 6 MHz. In this configuration, the static displacement of the tip of the resonator due to the light field amounts to 0.4 pm and the corresponding phase shift of the laser (the carrier) equals 0.2 mrad. This shift is easily observable as, for the 1 mW laser power, the shot noise limited phase resolution is 0.45 micro radian within the allowed detection time, before “hole-overburning” becomes non-negligible (approximately 16 ms for the 122 Hz linewidth). For comparison, a direct reflection of a 1 mW laser on the resonator would give rise to a much smaller static displacement (20 fm), justifying the efficiency of this dispersive approach.

Calculations also showed that the amplitude of the Brownian motion at 3K is 0.2 pm, and the spectral sidebands of the detection laser contain an integrated phase of 0.11 mrad due to this thermal excitation. For an integration time equal to the inverse of the thermal linewidth (25 micro seconds), the shot-noise limited phase-resolution is 14 micro radian. The thermally excited sidebands are therefore readily observed, even within such short integration time.

Moreover, by increasing the integration time up to the maximum before over-burning, it is possible to observe and measure accurately the detailed shape and size of the sidebands. Zero-point motion of the resonator, averaged over the measurement, induces a small excess integrated phase of 0.4 micro radian in the sidebands. As this value is close to the phase resolution achieved within the maximum integration time before hole-overburning, the shot noise limited resolution is therefore sufficient to observe the effect of the zero-point motion of the mechanical resonator. By using either dilution fridge or an active laser cooling mechanism (or a combination of these), the temperature can be lowered near a point where the thermal excitation does not hide the effect of zero point fluctuations. For example, at 30 mK, the zero-point fluctuation induces approximately 10^{-3} relative excess integrated phase over the effect of Brownian fluctuations alone. Such a deviation seems measurable, provided sufficient knowledge of the relevant parameters (temperature, Q factor,...). Several measurements at different temperatures may also be used to estimate the various relevant parameters with the necessary accuracy. Note that the resolution can be further increased by repeating the full hole imprinting and measurement sequence several times, or use optical repumpers to preserve the spectral hole. As the current setup is based on a 3K cryostat, the zero-point motion measurement are not immediately feasible, but we have here included the numbers as this is one of the next major modifications.

A potentially perturbing effect arises due to fluctuations of the laser power. As the static displacement corresponding to 1mW of laser power is approximately 0.4 pm, this laser power must be stable to within 10^{-4} to ensure a perturbation much smaller than the zero point fluctuations (approx. 1 fm), a power stability requirement well within reach of standard stabilization techniques. In addition, the laser frequency must also be carefully controlled. The zero-point motion induces a frequency shift of the ions closest to the edge of the resonator of approximately 37 Hz. The probe laser must therefore have a frequency stability substantially better than that, which is well within reach of nowadays commercially available ultra-high finesse Fabry-Perot cavity stabilized lasers (which typically have sub-Hz frequency stability). Note that probing the Brownian motion alone at 3 K exhibits a much less stringent frequency stability requirement at the sub-kHz level, and this will be one of the first measurements we plan to perform using the resonators. In order to anticipate the zero-point motion measurement, a new ultrastable cavity has recently been integrated in the setup, see section "Cryogenic and Optical setup for testing resonators".

Resonator fabrication

In practice, the fabrication of the bulk crystals (Eu^{3+}:Y_2SiO_5) is carried out by the CNRS-CP partners of the project. They have a long-standing experience in crystal design and growth as well as spectroscopic characterization, and are growing crystals, which contain europium ions with optimal performance in terms of lifetime and coherence properties. The bulk samples have dimensions of the order of millimeters. In order to reach deeper quantum regimes proposed within the NanOQTech project, crystals with micro- and nanoscale dimension are required. These designs can be realized by subsequently using Focused Ion Beam (FIB) techniques to shape the crystal. These steps have over the last year been successfully carried out at the NEEL institute (CNRS-IN), in collaboration with research-engineer Jean-François Motte, who is specialized in FIB techniques. The following sections will summarize this part of the project.

Calibrations

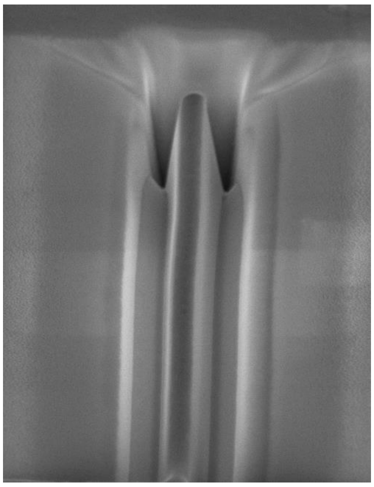

Figure 2 Resonator etched on the sides, but not liberated from below. Here, and in the following figures, the voltage used for imaging is 2.00 kV.

Before the beginning of the NanOQTech project, the FIB techniques had never been applied to Y_2SiO_5 or similar materials at the NEEL institute clean-room facilities, and little information was available in the literature. Thus, a major effort was required in order to calibrate the procedure and achieve a good etching efficiency. Figure 2 shows some of these initial trials. The spacing between the periodic structures is 1 μm. A standard gallium ion source was used and the ion energy applied was 30 kV. Due to the relatively low conductivity of the Y_2SiO_5 it was necessary to deposit a thin (20 nm) metal layer (aluminium) prior to etching the structures.

Initial trials

Once the calibration completed, we turned to the fabrication of the resonators. The major challenge was (and to some extent still is) to etch deep enough into the material in order to detach the resonator from below. This requires a large angle of the ion beam, and the ability to remove a large amount of material. As the etching rate is relatively slow (1 μm^3/nA/s) due to the fact that it is an oxide, and the extent of orientation of the sample relative to the ion beam is limited, this is a major challenge. Figure 2 shows an example of a resonator of which the contour lines have been easily etched, but illustrate the difficulty of liberating the resonator from below. In addition to the difficulty of removing material and obtaining the right angle, etching deep trenches are also problematic due to the fact that the metal layer (for removal of accumulated charges) becomes spatially separated from the etching points.

Liberation of resonator from below

In our initial attempts, the resonator was destroyed before (or at the same time) as we managed to liberate it from underneath, see figure 3, due to the challenges outlined above.

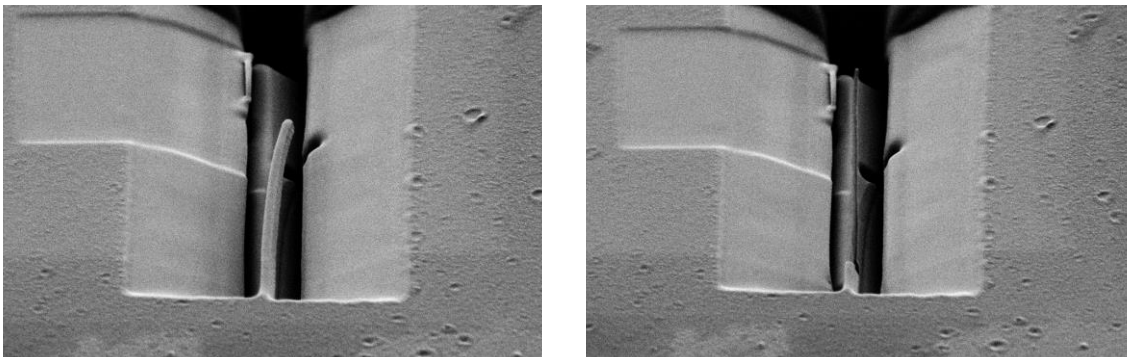

Figure 3 Initial test on resonator fabrication. The length of the resonator is approx. 2 μm long. The resonator breaks during an attempt to liberate it from below (second image).

In parallel with these initials trials, we progressed on the theoretical protocol, and realized that it would be preferable to work on somewhat larger resonators, as discussed in the section "Parameters obtained from simulations", on the order of 10 µm wide and 100 µm long. This also allowed us to do a part of the removal of the YSO material mechanically. More precisely, we placed a saw-cut (50 µm diameter wire close to the crystal edge, and starting from the saw cut, with a needle we could break away a large part of the material (between saw cut and resonator) before fine-etching with the FIB. Then we could take advantage of the edge of the crystal to constitute two sides of the resonator, and with the FIB create the other sides thanks to the access provided by the prior mechanical removal of material. This is illustrated in figure 4, where the resonator to the right has been achieved with this technique. The resonator to the left has been achieved using FIB alone, which rendered the fabrication more difficult, as the access to underneath from one of the sides was obstructed by the bulk material.

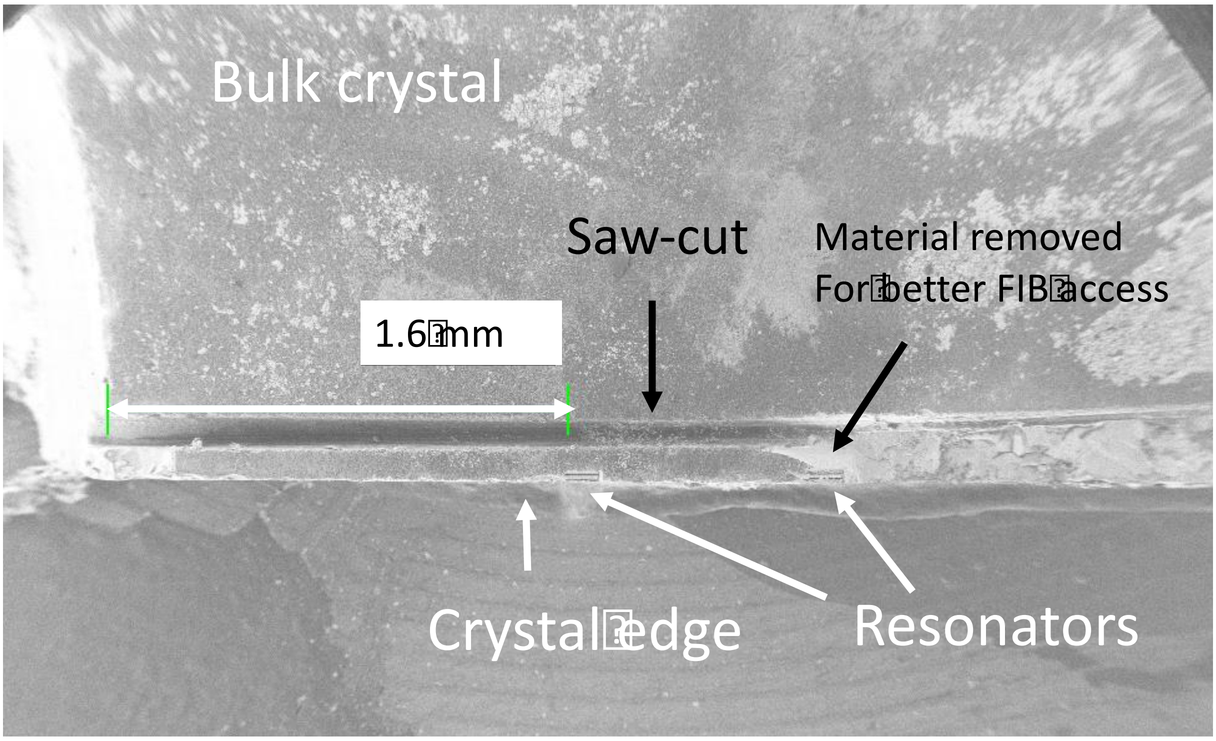

Figure 4 Overall view on crystal and saw cut. Two micro-meter scale resonators have been etched out of the bulk crystal.

A closer look on the resonator is shown in figure 5. Due to the fact that these are only initial trials, we have been working on unpolished crystals (polishing the crystals is very time-consuming) therefore the crystals and resonator appear with a rough surface.

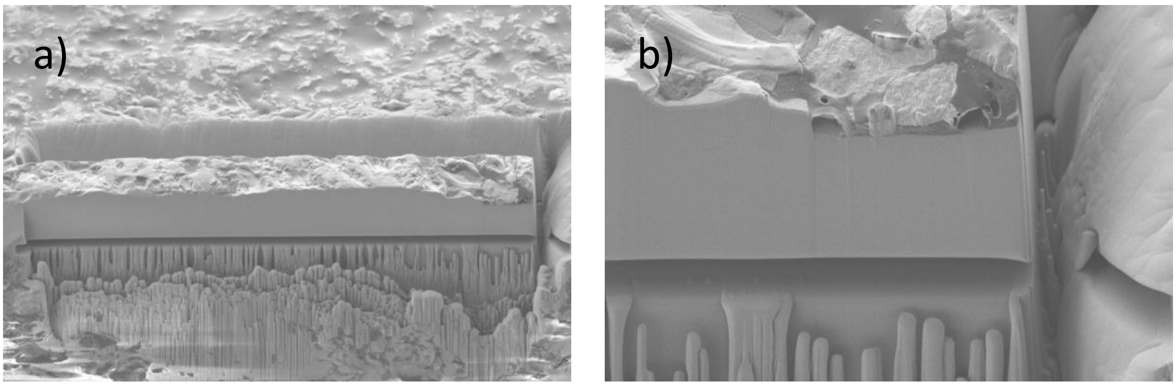

Figure 5 Zoom of the middle resonator from figure 4. In a) the full resonator (100 μm long, 10 μm thick) and b) a zoom on the tip.

In this manner, we were able to access the space below the resonator, and liberate the resonator from below. We also used the FIB on the upper surface of the resonator to remove a thin layer in order to obtain a smooth surface, see figure 6. This will allow us in the near future to test the resonator with limited light scattering. A small defect remains at the extreme tip of the resonator, but as this point is far from the laser-probing point, it is without consequences for preliminary measurements.

For the future resonators, given that most of the technical aspects of the technique are now mastered, we will work on polished crystals. Moreover, in these initials tests, the crystalline axes were randomly oriented relative to the resonator structure; in the next generation, we will also work on crystals which have been cut along particular crystalline axes, allowing the resonators to be oriented along these axes as to optimize the interaction with the probe laser beam.

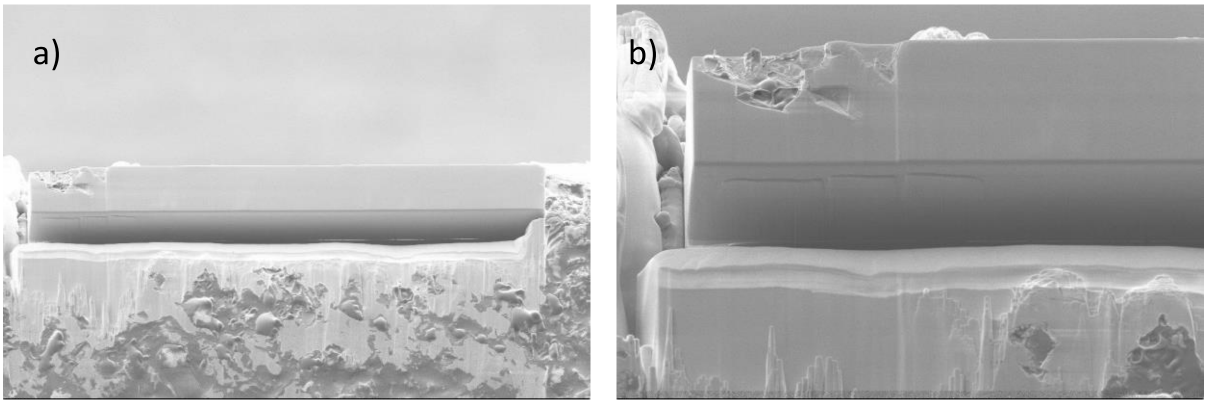

Figure 6 a) The same resonator as shown in figure 5 but with the surface polished with the FIB. b) A small defect remains on the tip of the resonator but does not affect probing.

As the fabrication procedure is independent of the orientation of the crystalline axes, aligning these axes relative to the resonator does not represent additional difficulties, and we expect to have new, aligned samples with increased absorption to test in the near future.

In addition to static images, we have tested the mobility of the resonator, by displacing it with a needle under the microscope inside the FIB chamber. A video is available on the NanOQTech website: https://www.nanoqtech.eu/ (see under News, 28 August 2017).

Cryogenic and optical setup for testing resonators

As stated above, the first prototype of the resonator is immediately available for measurements, and a second improved version is currently being fabricated. In order to thoroughly test these resonators, we need to excite the mechanical modes, couple them to laser light, and read out the phase shift of the laser. To perform these types of measurement, the resonators need to be cooled in a cryostat at 4 K. Due to the narrow linewidth of the transitions in the europium ions, and high strain-sensitivity, the cryostat needs to have an extremely low level of residual vibrations. Also, the laser light used to probe must be spectrally ultrastable.

Figure 7 Installation of a new ultrastable laser cavity in preparation for measuring mechanical resonators.

Therefore, in parallel with undertaking the fabrication of the resonators, we have been working in close collaboration with CNRS-SY in order to prepare the cryostat and lasers for the study of the resonator. In particular, NanOQTech Ph.D. student Nicolas Galland (CNRS-IN) has been strongly involved in the integration of a new ultrastable cavity for the lasers at CNRS-SY (see photo, figure 7) which will render these measurements feasible. Moreover, the cryostat which was currently used in another context at CNRS-SY has been adapted in order to eliminate vibrations, equally essential for the measurement of the resonators. More precisely, the crystal is mounted in a cylindrical copper block as shown in figure 8 (a). This cylinder was positioned on 3 beryllium-copper springs (1 cm long, 4 mm diameter) on the cold head of the cryostat. Thermal contact between the mounting block and the cold head was then realized with three groups of five annealed copper stripes (5 mm broad, 4 cm long, 200 μm thick each). Temperatures as low as 4 K have been reached in the vicinity of the crystal (as measured with calibrated thermistors). This extra stage of vibration isolation will prove sufficient to remove the residual mechanical perturbation from the cooling cycle and observe the spectral holes with in the resonators with for temperatures below 6 K. As proof of principle we have made preliminary measurement on bulk crystals (also obtained from CRNRS-CP). These preliminary measurements are shown in figure 8 (b). The modifications that have been realized are described in detail in an article recently published in Optics Express [7]. The article is published jointly with authors from three NanOQTech partners: CNRS-IN, CNRS-SY and CNRS-CP.

We still need to install a microscope objective inside the cryostat in order to investigate the resonators, as the light needs to be focussed to a spot size of 10 μm or less. The best solutions are currently being studied.

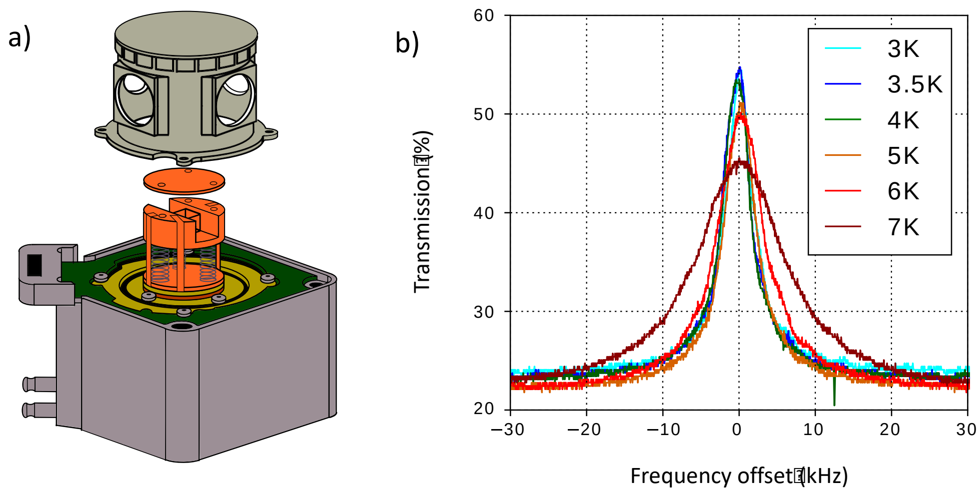

Figure 8 Schematics of the cryostat mount of the YSO crystal that prevents residual vibrations during the cooling cycle from disturbing atomic transition frequencies. The crystal mount itself is standing on three beryllium-copper springs that provide an extra vibration isolation stage. Thermal contact is realized by three groups of five annealed copper stripes. b) Transmission spectrum of a spectral hole corresponding to different temperatures of the crystal, using the cryostat mount depicted in a). The transmission percentage indicated takes into account the losses which are independent of the atomic absorption, caused by interfaces devoid of anti-reflection coating (the faces of the crystal in particular).

Conclusion

In the course of the last year, we have completed the design and fabrication of the first proto-types of mechanical resonators for the NanOQTech project, and made major improvements concerning the cryostat and optical setup in order to be able to study these resonators adequately.

Designing the resonators has required a detailed theoretical study, which has been completed in a close collaboration between three NanOQTech partners (CNRS-IN, CNRS-SY and AU). This study has enabled to determine the optimum geometry of the resonators, and make a quantitative study outlining the requirements concerning the optical setup.

The fabrication itself has been carried out at institute NEEL (CNRS-IN), starting from bulk crystals obtained from IRCP/Chimie ParisTech (CNRS-CP). It has involved preliminary characterization and optimization of Focused Ion Beam techniques on YSO crystals, and numerous trials before being able to liberate the resonator from underneath.

In conclusion, due to a very fruitful collaboration between 4 NanOQTech partners, the goals for this part of the project have been reached. Moreover, we have anticipated the necessary modifications of the optical setup, and we are thus confident that the next steps, i.e. performing the optics experiments with the resonators, can be done in optimum conditions.

Bibliography

[1] M. Aspelmeyer, P. Meystre and K. Schwab, Quantum Optomechanics, Physics Today, 65, 29 (2012)

[2] J. Chan, T. P. Mayer Alegre, A. H. Safavi-Naeini, J. T. Hill, A. Krause, S. Gröblacher, M. Aspelmeyer, and O. Painter, Nature 478, 89 (2011)

[3] J. D. Teufel, T. Donner, Dale Li, J. H. Harlow, M. S. Allman, K. Cicak, A. J. Sirois, J. D. Whittaker, K. W. Lehnert, R. W. Simmonds Nature 475, 359-363 (2011)

[4] I. Yeo, P.L. de Assis, A. Gloppe, E. Dupont-Ferrier, P. Verlot, N. S. Malik, E. Dupuy, J. Claudon, J.M. Gérard, A. Auffèves, G. Nogues, S. Seidelin, J.-P. Poizat, O. Arcizet, M. Richard Nature Nanotechnology, 9, 106 (2014)

[5] Fundamental Systems in Quantum Optics, edited by J. Dalibard, J. M. Raimond, and J. Z. Justin (Elsevier Science Publishers, 1992), Chap. Cavity Quantum Electrodynamics, les Houches session LIII.

[6] K. Mølmer, Y. Le Coq and S. Seidelin, Physical Review A 94, 053804 (2016)

[7] O. Gobron, K. Jung, N. Galland, K. Predehl, R. Le Targat, A. Ferrier, P. Goldner, S. Seidelin, and Y. Le Coq, Optics Express, 25, 15539 (2017)